ORIGINAL PAPER

Cooperative Catalysis: A New Development in Heterogeneous Catalysis

Jeong-Kyu Lee · Mayfair C. Kung · Harold H. Kung

Abstract Whereas cooperative effect in catalysis, in which multiple chemical interactions participate cooperatively to achieve significant enhancement in catalytic activity and/or selectivity, is common in enzymatic reactions, it has been sparingly employed in heterogeneous catalytic systems. Here, some recent literature examples of abiotic catalysis, with emphasis on heterogeneous systems, that employ cooperation between acid and base and two metal centers are briefly described to demonstrate the principles involved. Since effective cooperation places strict demand on the positions of the different functional groups, new synthetic methods and strategies are needed to design and construct structures useful for cooperative catalysis. Recent progress in our laboratory in synthesizing new nanocage structures that possess molecular-size cavities, atomic layer thick, porous shells with internal functional groups is described. These recent developments suggest possibilities of new catalytic transformations that have not been attempted before. This is illustrated with two speculative examples utilizing cooperative catalysis: oxidative hydrolytic desulfurization and terminal carbon activation of hydrocarbon molecules.

Keywords Cooperative catalysis

1 Introduction

Cooperative effect in catalysis (or cooperative catalysis), in which multiple chemical interactions participate

J.-K. Lee · M. C. Kung · H. H. Kung (✉)
Department of Chemical and Biological Engineering,
Northwestern University, Evanston, IL 60208-3120, USA
e-mail: hkung@northwestern.edu

cooperatively to effect significant enhancement in catalytic activity and/or selectivity, is common in enzymatic reactions. One well-known example is the enzyme serine endopeptidase. This enzyme catalyzes cleavage of a protein by hydrolysis of the amide bond. Although amide hydrolysis is acid-catalyzed, the peptidase functions effectively at near neutral pH, enhancing the reaction rate by as much as 10^6 time! How it works is rather well understood (Fig. 1) [1]. The active site is the hydroxyl of a serine unit, and the rate limiting step is the nucleophilic attack of the carbonyl carbon of the amide bond by the hydroxyl oxygen to form a negatively charged, carboxylate transition state. Thus, the rate would be enhanced with a more nucleophilic hydroxyl oxygen and if the charged transition state can be stabilized. As illustrated in the figure, hydrogen bonding (H-bonding) of this hydroxyl with a nearby imidazole group at the active site enhances the nucleophilicity of the hydroxyl oxygen. In fact, this effect is exaggerated by H-bonding of imidazole hydrogen with a carboxylate group further away, which increases the electron density of the imidazole. Additional stabilization of the transition state of the cleavage reaction is achieved by H-bonding interaction of the carboxylate with amino groups in the peptide backbone of the enzyme protein. Thus, in addition to the serine hydroxyl, at least four other groups of the enzyme protein participate cooperatively in the rate-limiting bond cleavage step, lowering the activation barrier and enhancing the reaction rate tremendously.

While ubiquitous in natural systems, there are only a handful of examples of cooperative effects in heterogeneous catalysis. At this point, we will first clarify the distinction between cooperative catalysis and bifunctional or tandem catalysis. Here, cooperative catalysis is used for catalytic phenomena in which chemically relevant interactions involving two or more groups act directly or
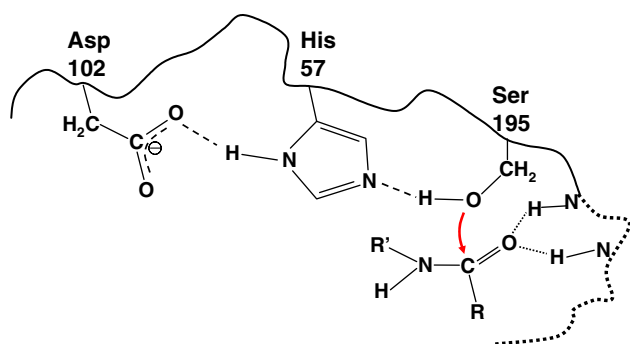
Fig. 1 Schematic drawing of serine endopeptidase showing cooperation among amino acid residues asp 102, his 57, and ser 195 to enhance the nucleophilicty of the hydroxy oxygen. The red arrow denotes nucleophilic attack of the hydroxy oxygen on the carbonyl carbon of the amide bond. H-bonding of two other amino groups with the carbonyl oxygen helps stabilize the transition state of the hydrolysis reaction

indirectly on the reacting molecule(s) in a chemical transformation steps. In contrast, bifunctional and tandem catalysis involve multiple transformation steps in a reaction sequence that are chemically independent, although the sequence order is important. For example, platforming is bifunctional catalysis in which an alkane molecule undergoes dehydrogenation, isomerization, and hydrogenation in sequence on different, non-interacting active sites. Likewise, shape-selective catalysis using zeolites makes use of size-exclusion and acid/base catalysis independently. They would not be classified as cooperative catalysis.

In this paper, we will briefly discuss a few examples in order to illustrate the rich opportunities offered by cooperative catalysis to improve activity and/or selectivity. The examples are mostly heterogeneous systems, but homogeneous catalysis is included. Not surprisingly, the concepts of cooperativity are similar, independent of the form of the catalyst. We will infer from these examples the need for catalytic structures that permit precise spatial positioning of specific functional groups. The discussion of these examples will be followed by a brief description of work in our laboratory to design and synthesize molecular size nanocage structures for catalysis. Finally, we will conclude with two speculative examples to demonstrate how to utilize cooperative catalysis to achieve reactions that have yet to be discovered.

2 Examples of Cooperative Catalysis

2.1 Cooperativity Involving Acid and Base Functions

Cooperative effect has been successfully demonstrated with the carbon–carbon bond formation between an electron-deficient carbonyl carbon and an electron-rich carbon

(Scheme 1). This reaction is facilitated by interaction of the electron lone pairs of the carbonyl oxygen with a Lewis acid to enhance the electron deficiency of the carbonyl carbon, and of the electron-rich carbon with a base to enhance its electron density. A specific example is the Henry's reaction, such as the addition of nitromethane to *p*-nitrobenzaldehyde (Fig. 2). Lin and coworkers found that a silica surface modified by a mixture of ureidopropylsiloxane (UDPS) and 3-[2-(2-aminoethylamino)ethylamino]propylsiloxane (AEPS) is much more active in catalyzing the reaction than a surface modified with either group or a physical mixture of two surfaces each modified by one group [2]. It was postulated that the ureido group functions as a Lewis acid by H-bonding to the carbonyl oxygen of the nitrobenzaldehyde, and the amino group of AEPS functions as a base and abstracts a proton from nitromethane (or at least form strong H-bonding with a methyl hydrogen). The activated nitromethane has an electron-rich carbon. Together, these interactions greatly facilitate the nucleophilic attack on the carbonyl carbon of nitrobenzaldehyde.

In aldol condensation, a carbon–carbon bond is formed between the α-carbon of a ketone and the carbonyl carbon of another molecule (Fig. 3). The reaction is facilitated by the cooperative effect of a Brønsted acid and a base. The Brønsted acid H-bonds with the carbonyl oxygen (or protonates it if it is a strong acid), making the carbonyl carbon more electron deficient. The base, on the other hand, H-bonds with the hydroxyl hydrogen of the enol form of the ketone and enhances the electron density at the α-carbon. Together, the Brønsted acid–base pair greatly enhances the rate of aldol condensation. This is demonstrated by Davis and his coworkers who tethered both propylamine and sulfonic acid groups onto a SBA-15 support, and showed that the solid catalyzes the condensation of acetone with *p*-nitrobenzaldehyde more effectively than solids containing only one type of functional groups [3]. These acid–base pairs must be in close proximity of each other in order to operate cooperatively. However, they must not neutralize each other either. Thus, one expects an optimal acid strength for the best catalytic effect. When Davis et al. compared three different tethered acid groups: benzylsulfonic acid, phosphonic acid, and
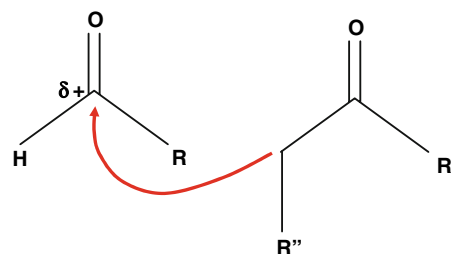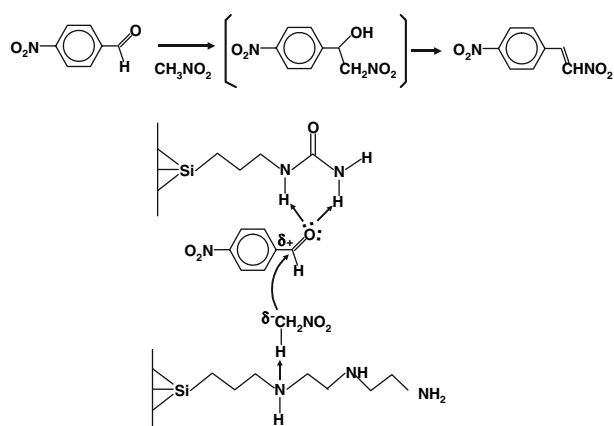

Scheme 1

Fig. 2 The addition of nitromethane to *p*-nitrobenzaldehyde is effectively catalyzed by cooperation between a tethered ureidopropyl group that functions as Lewis acid to render the carbonyl carbon more electrophilic, and an amino group that functions to enhance the nucleophilicity of nitromethane. The curved arrow indicates nucleophilic attack of the nitromethane on the carbonyl carbon. A surface tethered with both groups is catalytically much more active than a surface containing only one group

acetic acid, the activity decreases with increasing acid strength, which was explained as an indication that stronger acids are more likely to neutralize the neighboring amine.

Similar to aldol condensation, the Morita–Baylis–Hillman reaction involves the formation of C–C bond between a carbonyl carbon in an aldehyde and the α carbon of a ketone carbonyl (Fig. 4). Thus, the reaction would be facilitated by making the carbonyl carbon more electron deficient and the α-carbon more electron rich. Kwong et al. showed that, indeed, the reaction was greatly facilitated using a bifunctional polymer that contains a phenolic and a triphylphosphene group [4]. The phenolic proton functions as a Lewis acid and H-bond with the carbonyl oxygen of the reactant, increasing the electron deficiency of the carbonyl carbon, whereas the triphenylphosphine phosphorus
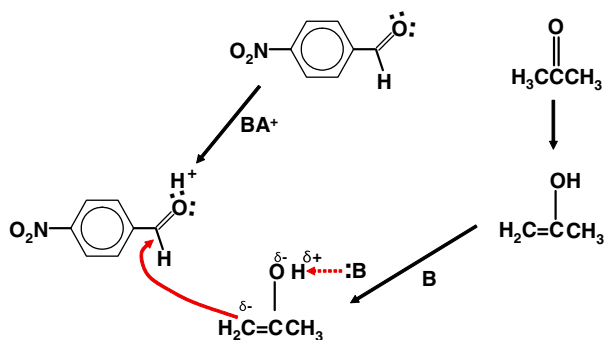
functions as a base to enhance the electron density of the α-carbon. Consistent with this picture is the observation that replacing the phenolic group with a benzyl alcohol group lowers the activity, suggesting that a more acidic proton is more effective.

2.2 Cooperativity Involving Metal Centers

It is common that metal ions in enzymes act as Lewis acid to activate substrates and generate nucleophiles. An example is the nucleases, which are very active in cleaving phosphate disaster bonds that are otherwise rather stable en vivo. Borrowing this concept, Livieri et al. synthesized a Zn complex that is active in cleaving the phosphate bonds in bis *p*-nitrophenyl phosphate (BNP) utilizing the cooperation involving two Zn complexes [5]. According to the proposed mechanism, the active center consists of a Zn ion coordinated to three N atoms: two in pyridine rings and one a secondary amine [6]. A hydroxyl groups is also attached to the amine ligand (Fig. 5). A water molecule can be coordinated to the Zn ion, and its interaction with Zn results in a low pKa of 6.68. Consequently, at neutral pH, the Zn-bound water is deprotonated. But the presence of a hydroxyl group nearby exchanges proton with the deprotonated bound water, and, at equilibrium, both monodeprotonated forms are likely to exist although the equilibrium is shifted to the hydroxide form. The water molecule bound to the alkoxide complex can be displaced by the anionic BNP which is further stabilized by H-bonding with a neighboring pridine 6-amino group. Coordination of the phosphate ester to the metal ion results in its activation towards nucleophilic attack by the alkoxide
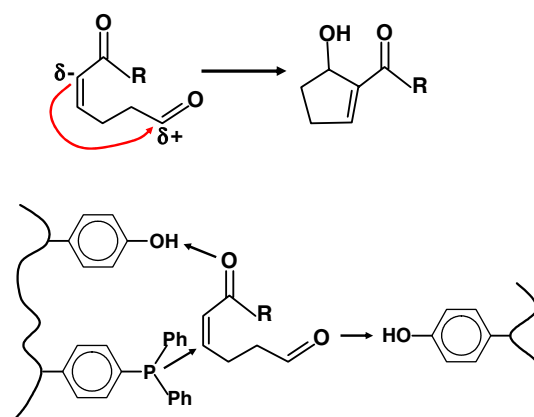

Fig. 3 In aldol condensation of nitrobenzaldehyde and acetone, H-bonding or protonation of nitrobenzaldehyde by a Brønsted acid enhances the electrophilicity of the carbonyl carbon, whereas H-bonding of the enol form of acetone with a base enhances the nucleophilicity of the α-carbon

Fig. 4 The Morita–Baylis–Hillman reaction (shown on top) can be facilitated by the cooperative effect of a phenolic group that H-bonds with the carbonyl oxygen of the aldehyde, making the carbonyl carbon more electrophilic, and interaction of a phosphine and another phenol group with the unsaturated ketone, making the α-carbon more nucleophilic

oxygen, and cleavage of one phosphate arm to form a mono *p*-nitrophenyl phosphate.

If another Zn complex is also present, then cleavage of the second phosphate arm can occur by similar activation of the Zn-bound, mono *p*-nitrophenyl phosphate. The cooperativity of two Zn complexes is further demonstrated by Martin, et al. who used third generation poly(propylene imine) dendrimers functionalized on the periphery with triazacyclononane-bearing acetate, which are known to be good ligands for Zn(II) ions to form active complexes for cleavage of phosphate esters [5]. By changing the density of the triazacyclononane, they could change the density of the Zn complexes on the dendrimer, and showed that the phosphate ester cleavage rate exhibited a second order dependence on the Zn complex density, indicating cooperation between the two Zn complexes.

The last example involves Ti metallocene complexes that are active catalysts for olefin polymerization. It was found that an isolated Ti complex (Fig. 6) is 50 time less active that two Ti complexes linked together by a–CH$_2$CH$_2$–unit in styrene polymerization [7]. The following explanation was offered. In a catalytic cycle, the polymer chain and the phenyl ring of the last inserted styrene are coordinated to the active Ti center. Because of steric crowding, the next styrene monomer can only coordinate to the Ti center by π-bonding with the C=C. However, in the case of a dimeric Ti center, the adjacent Ti atom can assist by π-bonding with the last phenyl ring of the growing polymer and freeing up a coordination site at the active Ti atom for the incoming monomer, or the phenyl ring of the incoming monomer and enhancing the binding of the monomer to the active Ti atom. Either way, binding of the monomer is enhanced, resulting in higher activity.

3 Construction of Cage-Like Catalytic Structures

The examples above illustrate the rich potential for superior performance in cooperative catalysis. However, effective use of cooperativity demands catalytic structures that could anchor the necessary functional groups at strategic positions and in an appropriate environment, such as hydrophobicity and hydrophilicity (sometimes also referred to as outer sphere). Since in cooperative effects, the various functional groups interact directly or indirectly with the reacting substrate molecule, it follows that these groups must be in close proximity to each other, within molecular dimensions. In nature, this is accomplished by building the enzyme protein one amino acid at a time, i.e., one building block at a time to form the desired structure. In homogeneous catalysis using coordination complexes, this would be attempted by covalently linking functionalized ligands with well-defined (length and composition) linker groups. Synthesis techniques for heterogeneous catalysts are less well developed. Typically, the different functional groups are randomly attached to a support, and cooperativity relies on statistical pairing of the functional groups (such as in the examples discussed above). In principle, it should be possible to control the separation between two functional groups with covalent linkage, similar to the technique used in homogeneous coordination complexes.

In recent years, we have undertaken two approaches to attack this challenge of controlled introduction of different functional groups. One approach is to develop a unit-by-unit technique to synthesize inorganic (siloxane) structures that would permit specific positioning of functional groups [8], and another is templated synthesis of nanocage structures of molecular dimensions which we will describe below.

Fig. 5 Proposed mechanism for the Zn-complex catalyzed hydrolysis of *p*-nitrophenyl phosphate. The overall reaction for bis *p*-nitrophenyl phosphate is shown on top
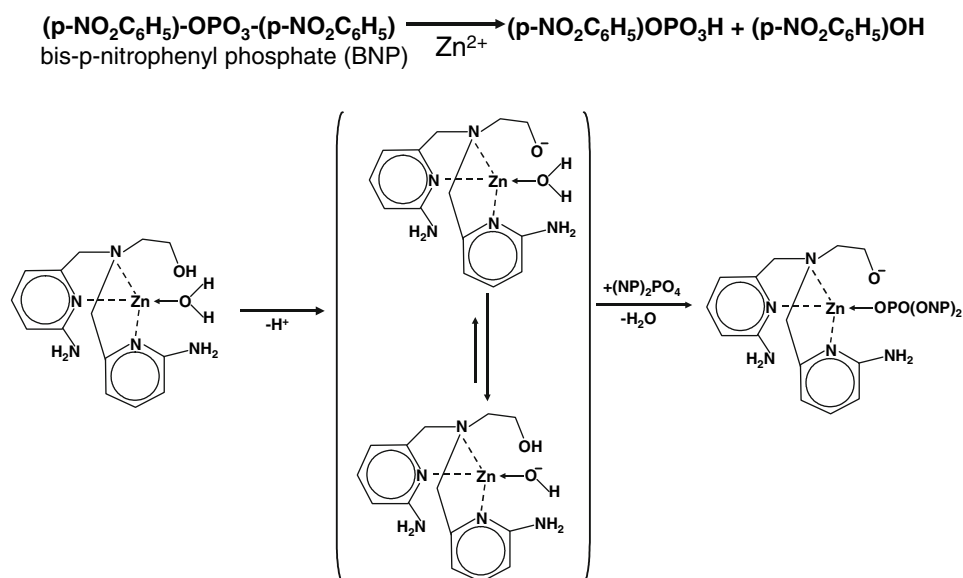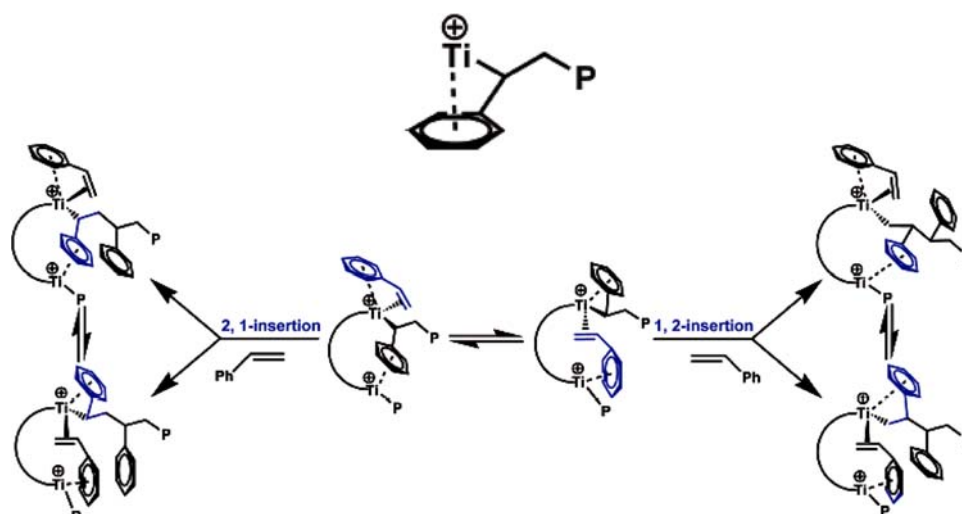
Fig. 6 In an isolated Ti metallocene complex for styrene polymerization, the growing chain and the phenyl ring of the last inserted monomer coordinate to the Ti atom, leaving only one free coordination site for an incoming monomer (top). When two Ti complexes are tethered close to each other, the second Ti atom can provide coordination site for the last phenyl group of the growing chain or the incoming monomer. This results in stronger binding of the incoming monomer because both the C=C and the phenyl ring can be coordinated to either of the Ti atoms. The net result is faster polymerization rate. (From reference 7, copyright National Academy of Sciences)

The goal to synthesize nanocage structures is inspired by the fact that in an enzyme, a protein is folded to form a spatial region of a size that accommodates the reactants, commonly referred to as a pocket, where a catalytic reaction takes place. The relevant functional groups are strategically placed in the pocket to effect cooperativity. One can formulate a set of desirable features for the nanocages for use in catalysis:

(a) The cavity should be of molecular dimension suitable for the target reaction and the corresponding reactants and products. Typically, this would be one to a few nm in size.

(b) The cage shell should be porous and one to a few atom-layer thick, so that diffusion of reactants into and products out of the nanocage is facile. The shell can also provide selectivity of the reactants based on size (size-selectivity) or other molecular properties (e.g., polarity).

(c) The interior wall of the shell should be functionalized with groups that are active for catalysis or can be converted into one.

(d) The distribution of components of the structure should permit introduction of different function groups at specified locations. This could be accomplished with a heterogeneous shell wall or incorporation of another structure inside the cage that has different functional groups. The latter could be a core molecule, for example.

There are reported syntheses of the cage structures in the literature, which are more appropriately termed hollow nanospheres. Typically, a spherical template is used which can be a micelle [9], a metal nanoparticle [10], block copolymer nanoparticles [11–13], or other degradable material. An organic or inorganic polymeric layer is then formed onto the template. Subsequent removal of the template results in a hollow nanosphere. Control of the thickness of the polymeric layer is difficult and the preparations generally result in structures with walls much thicker (by orders of magnitude) than a few atomic layers. Introduction of functional groups is accomplished by post-synthesis modification, and the ability to control their locations is very limited.

We aim our approach to permit formation of functional groups during the nanocage synthesis process, thus dictating the number and location of these groups. Another key feature is the shell cross-linking procedure which results in much thinner shells with the possibility of controlling the access window size–a property that we have yet to explore. At present, we have succeeded in preparing nanocage structures of the desired dimensions (2–5 nm diameter) and with functionalized interior shell walls. However, further research is needed to incorporate all of the desirable features listed above.

Our first generation of nanocages was synthesized with a shell cross-linked micelle templating method shown in Fig. 7 [14]. Briefly, a surfactant molecule (triethoxysilyl)propylcetylcarbamate **I** was synthesized that possesses a polar headgroup and a long, hydrophobic hydrocarbon tail. It forms a micelle **II** of about 2 nm diameter in ethanol (step i), and contains a carbamate group that can be cleaved and converted to an amine group. The alkoxysilyl head

groups of the surfactant, after hydrolysis to silanol with an ethanol–water mixture containing HCl, subsequently condense to form cross links. Further cross-linking is accomplished by reacting the remaining silanol groups with dimethyldimethoxysilane, and the remnant isolated silanols are capped with trimethylmethoxysilane to form a shell cross-linked micelle **III** (step ii). The transformations in these reactions are quantitative, as indicated by ^{1}H NMR. **III** is soluble in ethanol, and retains the 2 nm size (as determined by dynamic light scattering). Very importantly, upon changing solvent from ethanol to a more hydrophobic mixture of ethanol/toluene (1:1), the cross-linked **III** is robust and retains its structure, whereas micelle **II**, without cross-linking, disintegrates.

The final shell cross-linked nanocage **IV** is generated by treatment of **III** with trimethyliodosilane to effect cleavage of the carbamate bond, followed by addition of methanol and purification (step iii) to form tethered amines. Since the hydrophobic hydrocarbon tails in **III** are interior to the siloxane shell, the silylpropylamine groups generated would be tethered to the interior surface of the shell in **IV**, as depicted schematically in Fig. 7. Formation of **IV** was confirmed by MALDI-TOF, ^{1}H and ^{29}Si NMR, DLS, and TEM. In fact, Z-contrast high resolution electron micrographs of **IV** stained with W or Mo showed spherical objects of about 2 nm that contain both Si and W or Mo atoms.

Since the amine groups are interior to the nanocage, they can only interact with molecules smaller than the pores on the shell. Indeed, we found that they respond positively to the ninhydrin test (a classical test for amines) but do not interact with the much larger ZnTPP prophyrin molecules. Finally, we determined that they are catalytically active, and decompose 3-oxobutanoic acid about seven times faster than a corresponding free amine in solution, and produce a majority of hemiacetal and acetal as initial products, instead of acetone as in the case of free amine. Thus, these nanocages exhibit confinement effects.

Although we succeeded in forming nanocages of this type, our experience also exposed the limitation of this synthetic method. Specifically, it is not easy to change the size of the nanocage substantially, and there is limited flexibility in introducing different functional groups into the structure. Furthermore, micelles can only exist in very dilute solution, thus limiting the yield of nanocages. Therefore, we proceeded to investigate a new synthesis strategy–the dendrimer-directed synthesis.

The concept behind the dendrimer-directed synthesis method is similar to micelle templating, except that an immolative dendrimer is used instead of a micelle. An immolative dendrimer is made of subunits linked with immolative bonds. Upon cleaving these bonds at the end of the synthesis, the resulting small subunits could diffuse through the cross-linked shell, leaving a cage-like structure behind. The periphery (end groups of the branches) of the dendrimer is functionalized such that these groups can cross-link either directly with each other or with a cross-linking agent to form an atomic-layer thick, porous shell. The cleaved immolative bonds attached to the peripheral groups would leave functional groups behind that are

Fig. 7 Schematic drawing showing the steps in the synthesis of a 2 nm-diameter siloxane nanocage **IV**, containing propylamine groups tethered to the interior surface of an atomic layer-thick, cross-linked siloxane shell, derived from a micelle of (triethoxysilyl) propylcetylcarbamate **I**. The inserts for **III** and **IV** are 2-D cutout representations of the cross-linked shell. (Adapted from ref. [14], copyright American Chemical Society.)
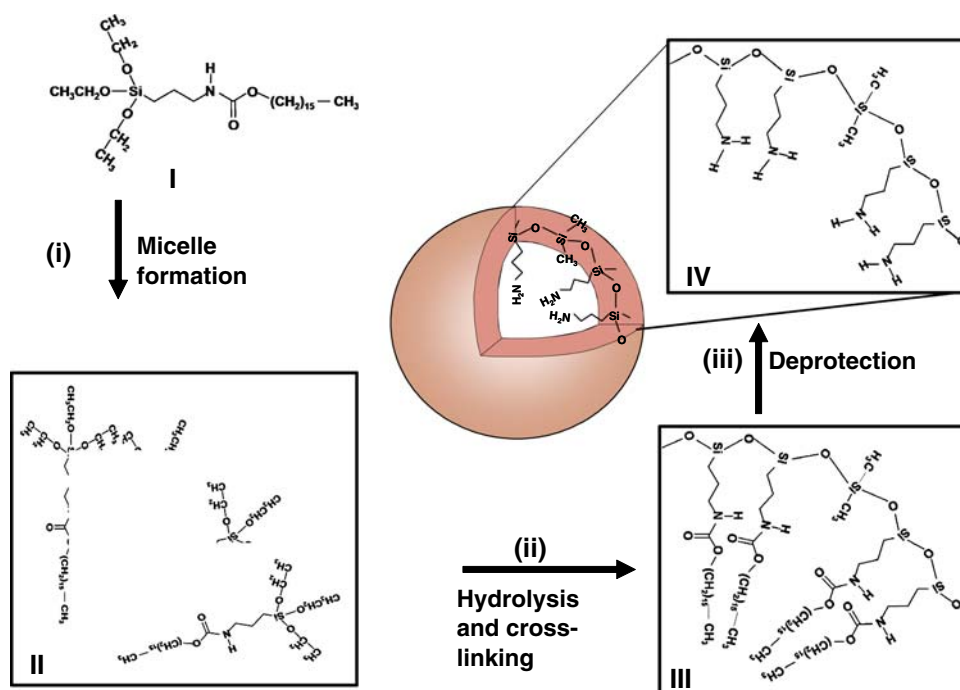
tethered to the cross-linked shell. Finally, the dendrimer core can be designed to be left encapsulated in the cage and to possess specific functional groups.

The structural uniformity provided by dendrimer templates marks a significant advancement in the degree of molecular control of the second generation relative to the first generation nanocages. As a molecule of well-defined stoichiometry, the size of a dendrimer is determined by its composition and the generation number. Consequently, the cavity size of a nanocage is uniform and can be adjusted over a wide range. It is noteworthy that dendrimers are typically 2–6 nm in diameter. Thus, we can form nanocages with uniform-size cavities in the molecular size range.

There are different reaction schemes to synthesize dendrimers, depending on the chosen immolative bonds. Figure 8 shows the scheme for a fourth generation dendrimer containing immolative carbamate bonds that we have used [15], and its further conversion into a nanocage [16]. In this scheme, we chose a combination of convergent and divergent growth method to form a generation 4 (G4) dendrimer **V**. This dendrimer has 96 surface olefinic groups to anchor the shell cross-linking agent 1,4-bis(dimethylsilyl)benzene by hydrosilylation. The dendrimer was characterized with ^{1}H, ^{29}Si, and ^{13}C NMR. Very importantly, MALDI-TOF results showed that pure dendrimer was obtained. DLS results were also consistent with the expected diameter of 4.3 nm, as were the TEM images.

After shell cross-linking, the molecular weight and the diameter of these structures increased and the characterization results suggested the formation of a shell that averages 2–3 nm thick, consistent with the chemistry shown in the figure. After cleaving the carbamate bonds, the resulting structure retains a DLS hydrodynamic size of about 10 nm, and TEM images of a sample stained with OsO_4 show structures 5–10 nm in diameter that contain both Os and Si (as determined by single particle EDX). Thus, we have synthesized the nanocage structure as indicated. Finally, cleavage of the carbamate linker bonds would generate hydroxyl groups tethered to the interior shell wall. The presence of the hydroxyl groups has been detected by their reaction with *p*-nitrophenyl chloroformate, which can be followed by UV–vis spectroscopy. Application of this second generation nanocage in catalysis is being investigated, and the results will be reported in the future.

4 Speculative Examples of New Reactions Utilizing Cooperative Catalysis

The successful synthesis of nanocage structures offers the potential of designing multifunctional catalysts, where designated functional groups are positioned at specific locations, for cooperative catalysis to effect reactions that have not been possible before. We offer two such examples conceptually without specifying the details.

One example is desulfurization of thio-compounds by oxidative hydrolysis. Currently, desulfurization is accomplished by hydrogenolysis of the C–S bonds in the well-established hydrodesulfurization process. Although the process is very effective in removing sulfur, it consumes hydrogen, and the selectivity for desulfurization without hydrogenation of the unsaturated hydrocarbon is often a challenge. An alternative would be hydrolysis of the C–S bond to form an alcohol (Fig. 9), but the reaction is thermodynamically unfavorable. Removal of sulfur by oxidation is thermodynamically favorable, but selective insertion of oxygen into the C–S bond without also oxidizing other C–C or C–H bonds (i.e., undesirable oxidation reactions) is also challenging.

One possible alternative is to cleave the C–S bond by hydrolysis, while simultaneously form a S–M bond (M a metal ion) to provide the thermodynamic driving force. The S is then removed in a subsequent step with oxygen to form SO_2. Since both reactions can be carried out at low temperatures, this process may selectively remove sulfur without consuming the valuable hydrogen. A possible catalyst is shown in Fig. 9. A metal cation is available to interact with the electron lone pair on the S atom and, by induction, decreases the electron density at the carbon atom in the C–S bond. At the same time, a basic site enhances the electron density of an O atom in a hydroxyl group by H-bonding. The more nucleophilic O atom attacks the electron deficient C atom, cleaving the C–S bond, and the S atom is bonded to the metal center. The S atom is then removed by oxidation with oxygen, regenerating the active site (not shown).

Another example is activation of the terminal carbon of an alkane. Since secondary and tertiary carbenium ions and radicals are energetically more favorable than their primary counterparts, reactions in which the transition state has either a cationic or radical character would result in activation of the internal carbon atoms. It follows that if the transition state has an anionic character, preferential activation of the terminal carbon might be possible. Presumably, if the C–H bonds of the terminal carbon can interact with electron-donating basic groups through H-bonding, these C–H bonds would be polarized, resulting in an electron-rich carbon atom that would be more favorable at the terminal than the internal position (Fig. 10). If an electrophile (X) is available nearby, the formation of a C–X bond would be facilitated, and terminal activation could be achieved. This hypothetical scheme would require cooperation among different groups interacting with the reactant molecule simultaneously.
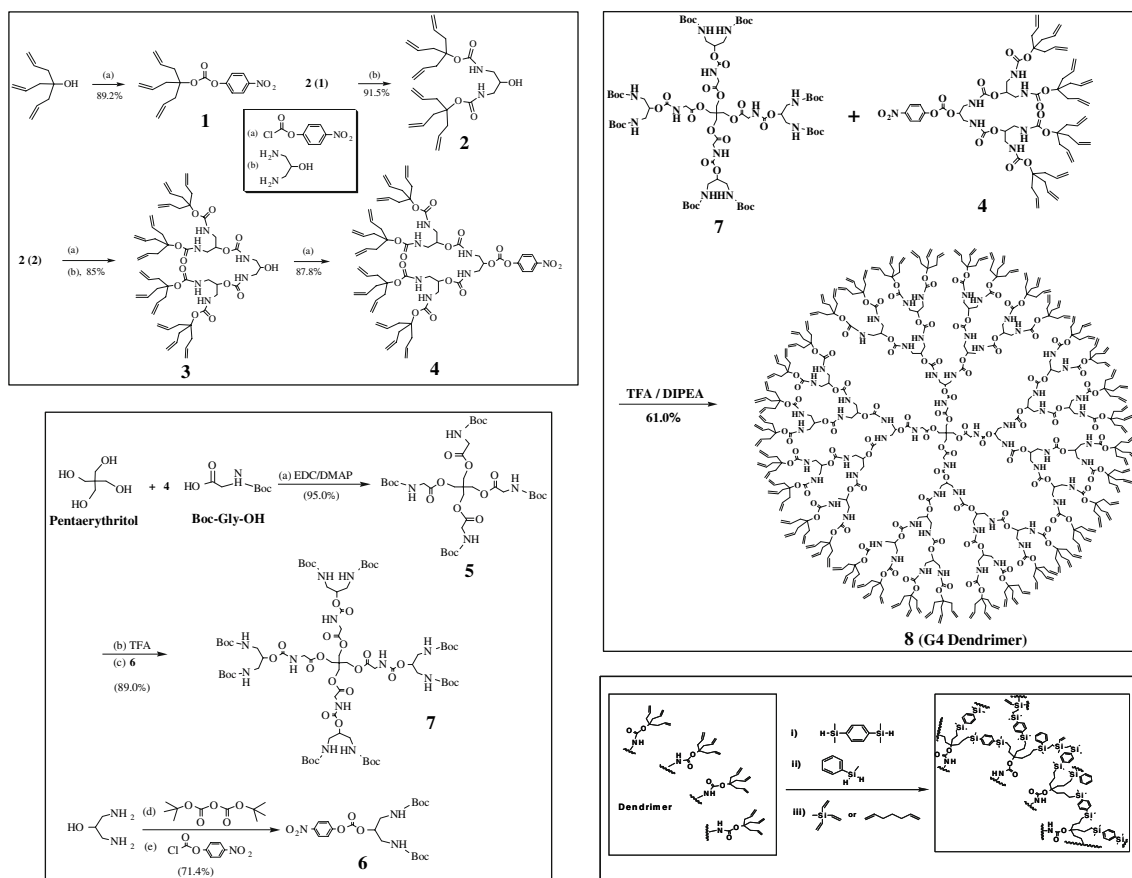
Fig. 8 Synthesis of a shell cross-linked generation 4 (G4) carbamate dendrimer. Top left panel shows the convergent synthesis of a G2 dendron starting from 2-methyl-3-buten-2-ol. Bottom left panel shows the divergent synthesis of the G2 core starting from pentaerythritol. The G2 dendron and the G2 core are coupled as shown in the top right panel to form a G4 dendrimer. Shell cross-linking of this G4 dendrimer is shown in the bottom right panel, using 1,4-bis(dimethylsilyl)benzene as the primary cross-linking agent, and a combination of methylphenylsilane and methyltrivinylsilane or heptadiene to complete shell cross-linking
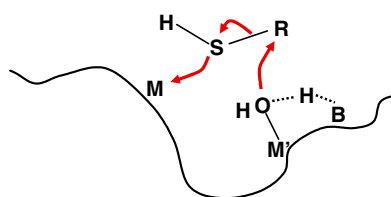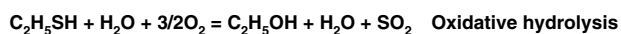
$$C_2H_5SH + H_2O = C_2H_5OH + H_2S \qquad \textbf{Thermodynamics unfavorable}$$

$$C_2H_5SH + 3/2O_2 = C_2H_5OH + SO_2 \qquad \textbf{Oxidation not selective}$$

$$C_2H_5SH + H_2O + 3/2O_2 = C_2H_5OH + H_2O + SO_2 \qquad \textbf{Oxidative hydrolysis}$$

Fig. 9 A conceptual reaction center for oxidative hydrolysis of a C–S bond, involving cooperativity of two metal centers and a basic group. See text for details

Fig. 10 A conceptual reaction scheme for activation of a terminal carbon of a hydrocarbon molecule, involving H-bonding with three basic sites and interaction with an electrophile. See text for detail

5 Conclusion

Although common in enzymatic reactions, cooperative catalysis has only been recently investigated and utilized in heterogeneous catalysis. When properly applied, it can lead t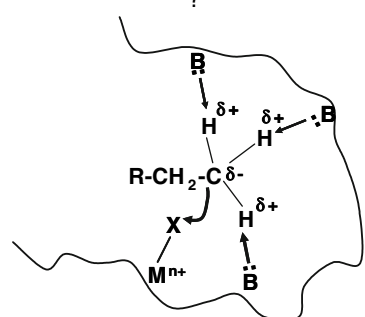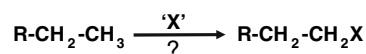o very significant increases in activity, as demonstrated in the illustrative examples described above. It can also lead to enhanced selectivity, although this imposes a more stringent requirement of the cooperative action of the functional groups. Thus far, the literature results show very promising possibilities. When coupled with advances in

synthetic know-how, especially in the synthesis of macro-molecules, it becomes increasing possible to design catalytic structures for targeted reactants and reactions, making use of cooperativity among multiple functionalities within the structure to conduct highly demanding reactions that have not been possible before. Although the synthesis steps are still rather demanding at present, one could expect that future advances would lower the barrier such that one day, catalysts by design will become truly a reality, and highly efficient catalytic transformations will be a norm instead of a stretched goal, much like what nature has been practicing for millions of years.

References

1. Voet D, Voet J (2004) Biochemistry, vol 1. John Wiley & Sons, New York
2. Huh S, Chen H-T, Wiench JW, Pruski M, Lin VS-Y (2005) Angew Chem Int Ed 44:1826
3. Huh S, Chen H-T, Wiench JW, Pruski M, Lin VS-Y (2005) Angew Chem Int Ed 44:1826
4. Zeidan RK, Hwang S-J, Davis ME (2006) Angew Chem Int Ed 45:6332–6335
5. Kwong C, Huang R, Zhang M, Shi M, Toy P (2007) Chem Eur J 13:2369–2376
6. Martin M, Manea F, Fiammengo R, Prins L, Pasquato L, Scrimin P (2007) J Am Chem Soc 129:6982–6983
7. Livieri M, Mancin F, Saielli G, Chin J, Tonellato U (2007) Chem Eur J 13:2246–2256
8. Li H, Marks TJ (2006) Proc Natl Acad Sci 103:15295–15302
9. Xue W, Kung MC, Kung HH (2005) Chem Comm 2164–2166
10. Zhang Y, Jiang M, Zhao J, Zhou J, Chen D (2004) Macromolecules 37(4):1537–1543
11. Chen J, Wiley B, Li Z-Y, Campbell D, Saeki F, Cang H, Au L, Lee J, Li X, Xia Y (2005) Adv Mater (Weinheim, Germany) 17:2255–2261
12. Huang H, Remsen EE, Kowalewski T, Wooley KL (1999) J Am Chem Soc 121(15):3805–3806
13. Sanji T, Nakatsuka Y, Ohnishi S, Sakurai H (2000) Macromolec 33(23):8524–8526
14. Cornelissen JJLM, Connor EF, Kim H-C, Lee VY, Rice MP, Volksen W, Sundberg LK, Miller DR (2003) Chem Commun 8:1010–1011
15. Suh Y-W, Kung MC, Wang Y, Kung HH (2006) J Am Chem Soc 128:2776
16. Lee J-K, Suh Y-W, Kung MC, Downing CM, Kung HH (2007) Tetrahedron Lett 48:4919
17. Lee J-K, Kung MC, Suh Y-W, Kung HH (2008) Chem Mater 20(2):373–375